CNT ENABLED FABRIC SENSORS FOR MONITOR RESIN INFUSION AND CURING OF COMPOSITES

ZHAI Yujiang[1], WANG Guantao[1,2], WANG Yong[1], LUO Sida *[1,]

[1] School of Mechanical Engineering & Automation, International Research Institute for Multidisciplinary Science, Beihang University, Beijing, 100191, China
[2] Center of Safety Research, School of Engineering and Technology, China University of Geosciences, Beijing, 100083, China.

Keywords: self-sensing composites, CNT sensors, smart fabrics, process monitoring

ABSTRACT

High performance polymeric composites need to have built-in functionality to continually monitor and diagnose their own health states. In this work we present a novel strategy for in-situ monitoring the processing stages of composites by braiding CNT-coated fiber bundles into the fabric reinforcing layers. The CNT fabrics, assembled through by a cost-effective, swift and continuous dipping/drying method, are highly sensitive to monitor and quantify different events of composite manufacturing, including resin infusion, crosslinking, gelation, and degree of curing. By varying curing temperature and resin formulation, different curing kinetics can be accurately derived using the smart fabrics. More importantly, distribution of local information of the composites can also be achieved in real time upon wisely configuring a scalable sensor network. After manufacturing, the smart fabrics which are readily and non-invasively integrated into composites can provide life-long structural health monitoring of the composites, including detection of deformations and cracks.

1 INTRODUCTION

Fiber-reinforced polymeric composites (FRPs) are traditionally important as structural materials for a wide variety of applications such as commercial & battle aircrafts, jet engine, wind turbine, gas and oil transmission pipelines etc.. Since the last decade, substantial attention has been paid for the research and development of next generation of FRPs with built-in multifunctionality for self-sensing, identifying, quantifying and deciding their own health states [1-2]. Different approaches were attempted to impart the FRPs with capabilities for structural health monitoring (SHM) during different stages of their life cycle [3-4]. As compared to the traditional methods, carbon nanotubes (CNTs) enabled in-situ SHM technology has attracted a considerable amount of attention by virtue of their excellent mechanical robustness, non-invasive embeddability and conformability, light weight, low cost in fabrication and implementation, and remarkably high piezoresistive sensitivity [5-6]. Different types of CNT sensors have been explored, e.g., by bridging CNTs onto fiber and matrix interface as 1D sensors [7-8], by depositing CNTs to formats of thin films or buckypapers as 2D sensors [9-13], or by distributing CNTs directly in the resin matrix to form 3D sensors [14-15]. In most cases, the working principle of CNT sensors relies on the tunneling resistance change of the percolated CNT network upon external stimulus to impart the sensors with the capability for monitoring different mechanical deformations, cracks and failure modes in hierarchical composites [16-17]. In addition to monitoring the health state of the FRPs in their service stage, it is equally important to be able to in-situ and in-line monitor the resin infiltration and curing kinetics in manufacturing process of composites. Because of the complicated fibrous preforms, resin infiltration is always non-uniform and hard to predict its behavior. This may introduce problematic flow defects such as dry spots [18]. Aiming to resolve these issues, Zhang et al. used electrophoretic method to fabricate CNT coated glass fiber for probing the curing process of epoxy resin [19]. By taking advantage of the unique porous structure of CNT and graphitic nanoplatelet (GNP) thin films, our group invented the CNT and GNP thin film based fiber sensors for in-situ monitoring the manufacturing process of fiberglass prepreg laminates to sense resin infiltration and shrinkage [20-21].

Given the progress being made, however, there is still a lack of a highly sensitive, reliable and scalable method for large-area monitoring the manufacturing stage of hierarchical composites. We report here a novel strategy in developing smart fabrics comprised of co-braidable, scalable and designable CNT fiber sensors, which can be fabricated through a cost-effective and high-efficient dip coating process. The smart fabrics can be used as one layer of the woven roving performs. As such, it is able to be readily integrated into a composite structure through the well-developed vacuum assisted resin transfer molding (VARTM) technique. The smart fabrics could provide a precise way to monitor and quantify various events occurred during the composite manufacturing stage, including resin infusion, gelation as well as curing kinetics. The most distinctive feature of our smart fabrics is the built-in multiple fiber sensors that can serve as a sensing network to be incorporated and assembled into composites for large area sensing.

2 EXPERIMENTAL

CNT dispersion was prepared by dispersing 100 mg MWCNT (General Nano LLC.) in 200 mL of deionized water with 5 mL of nonionic surfactant triton X-100 (Sigma-Aldrich) in an ice bath using a Misonix 3000 probe sonicator (20 kHz). The sonicator was operated in a pulse model (on 10 s, off 10 s) with the power set at 45 W for 1 h. The length and diameter of CNTs in the resulting dispersion were characterized using preparative ultracentrifuge method (PUM) with the Optima MAX-XP ultracentrifuge (TLA-100.3, 30° fixed angle rotor, 13000 g-force, Beckman Coulter Inc.) and Delsa Nano C particle size analyzer (Beckman Coulter Inc.). To fabricate smart fabrics, a fiberglass roving extracted from the woven fabrics (part # 223, Fibre Glast Developments Corp.) was used as the substrate of fiber sensors. Depending on different requirements, single or five parallel fiber sensors were incorporated in the smart fabric. The structures of CNT coating were examined by scanning electron microscopy (SEM), energy-dispersive X-ray (EDX) and Raman spectroscopy. SEM was performed with JEOL 7400 at 10 kV for examining the morphologies of the smart fabrics. The same instrument was used to acquire the EDX to determine the carbon content of sensors. A Renishaw inVia Raman microscope was used for collecting the Raman spectra of the smart fabric sensor with a 785 nm excitation laser at a power of 1 mW.

The VARTM process was used to fabricate the composite laminate with embedded smart fabrics. Without specific notification, total of four layers of square shaped fabric (15 cm × 15 cm) were stacked into a multilayer composite preform. For single sensor experiments, the smart fabric layer was placed on top with the sensor parallel to the resin flow direction. For sensor array experiments, two smart fabric layers with five embedded sensors were respectively placed on top and at the bottom. The top (bottom) layer has the sensors parallel (vertical) to the resin flow direction. Subsequent to sensor integration and preform stacking, the fibrous stack was then placed in a vacuumed plastic bag to induce the resin infusion and curing process. The VARTM process was operated under one standard atmospheric pressure (0.1 MPa). Then the mixture of vinyl ester resin (part # 1110, Fibre Glast Developments Corp.) catalyzed by methyl ethyl ketone peroxide (MEKP-925, Norac, Inc.) with a certain mixing ratio was introduced to fill the vacuum bag. The total processing was isothermally maintained for 24 h. Subsequently, the composite laminate was debagged. To monitor the process of composite manufacturing, the resistance of embedded sensors was recorded by a Keithley 2401 Sourcemeter controlled by a homemade LabVIEW user interface during the whole curing process [22-23]. The curing temperature during each process was tested by a FLIR E40 thermal imaging camera.

3 RESULTS AND DISCUSSIONS

3.1 Fabrication, Integration and Characterization of Smart Fabrics

The smart fabrics included composite parts were prepared by three steps, i.e., fabrication of CNT enabled fiber sensors, formation of smart fabrics, and composite molding. Figure 1a shows the smart fabrics prepared by manually co-braiding the as-prepared fiber sensors into a woven roving cloth. During VARTM, the electric signal of fiber sensors embedded in the smart fabrics was simultaneously recorded to evaluate its capability for in-line monitoring resin infusion and curing of composites. The

smart fabrics technology is scalable to incorporate multiple fiber sensors as sensing network to cover large area SHM of composites. For demonstration purpose, the largest smart fabrics specimen we made was ~300 cm2 with a 5×5 sensor array (Figure 1a).

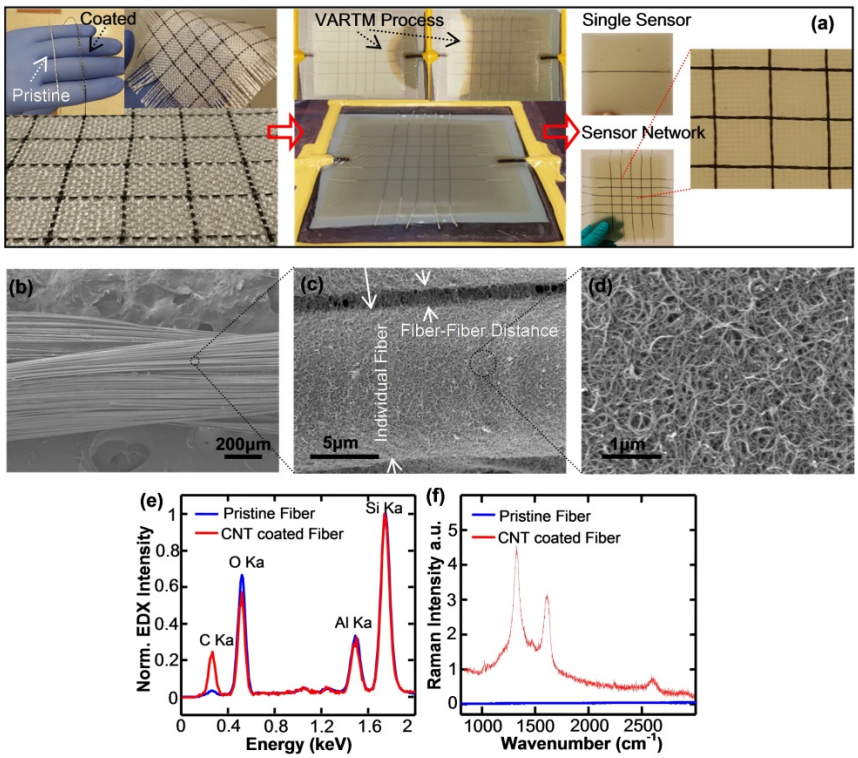

Figure 1. (a) Photographs of key steps in assembling the smart fabric integrated in composites; (b-d) SEM images of fiber sensors at different magnifications for examining the MWCNT packing structures on the fiber roving substrate; Comparison of (e) EDX and (f) Raman spectrum of a neat glass fiber roving and a MWCNT coated fiber sensor.

To characterize the CNT structure coated on the fiber core, a variety of microscopy and spectroscopy methods have been used. SEM images provide detailed evidence of CNT coating as shown in Figure 1b, 1c (low magnification) and 1d (high magnification). Albeit the small diameter of an individual fiberglass filament (~20 μm), the CNT nanoparticles were successfully coated on the fiber surface. Similar morphologies can also be found for the CNT coating on a large-area 2D substrate [24-25]. To further examine the successful coating of CNT on a glass fiber, we performed energy-dispersive X-ray (EDX) and Raman spectroscopy measurements on the fiber prior to and after the CNT coating. Upon normalizing to the silicon peak intensity, the EDX spectra (Figure 1e) clearly show that the carbon peak is substantially increased from 5.77 wt.% to 22.24 wt.% upon CNT coating. Similarly, the signature Raman features (Figure 1f) of MWCNTs, i.e. G-band around 1600 cm-1, D-band around 1300 cm-1 and 2D-band around 2600 cm-1, confirm the CNT coating process. According to the experimentally determined sedimentation function and subsequent model fitting [26-27], we calculated the averaged length (1845.2 nm) and diameter (3.74 nm) of MWCNT bundles in the dispersion. Based on weight measurements, the CNT content is determined to be less than 0.5 wt.% of the fiber sensor.

3.2 Sensing Capability of Smart Fabrics for Process Monitoring

Smart fabrics with a single fiber sensor have been studied principally to establish and quantify its sensing capability for monitoring resin infusion and curing of composites. To specify, the fiber sensor with equal length in the fibrous ply was placed parallel to the direction of the resin infusion. To study its capability, real-time resistance signal of a representative smart fabric sensor was demonstrated in

Figure 2. By monitoring resistance change (dR/R0) of the single fiber sensor embedded in smart fabrics, a rapid increase of dR/R0 from 0 to ~11(0 –6 min) was accordingly observed and it was then smoothly merged into a milder increase (6 – 28 min) approaching to a stabilized value of ~16 (highlighted in blue). Subsequently, this maximum dR/R0 value was kept almost constant from 28 min to 55 min (highlighted in green). As the continuity of the process, a pronounced decrease of dR/R0 from ~16 to ~7 was initially observed (1 h– 3 h) and then gradually leveled off to a plateau value of ~4 toward the end of the process (3 h to 24 h, highlighted in red).

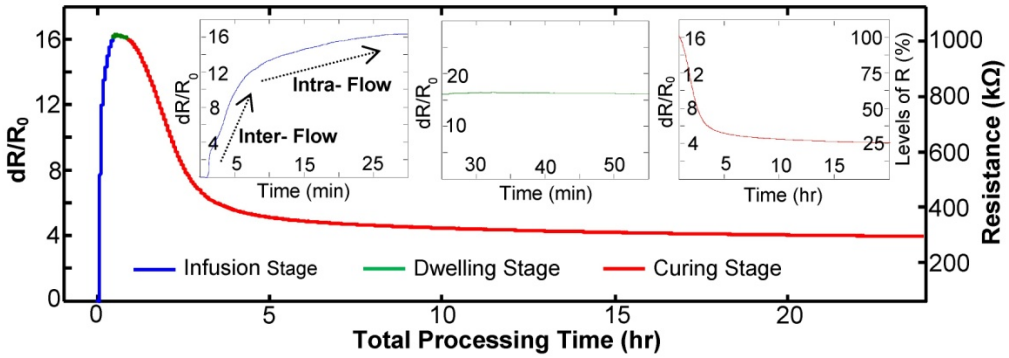

Figure 2. Resin infusion and curing process of hierarchical composites registered by the real-time resistance change of the embedded smart fabric sensor. Infusion stage: 0 – 28 min (blue curve); Dwelling stage: 28 min – 55 min (green curve); Curing Stage: 55 min – 24 h (red curve).

By correlating the resistance changes with physical states in composite manufacturing, it is interesting that the high repeatable trends of the sensor signal described above mimic closely to the whole curing progression. First, as resin injecting and wetting the fibrous preform with fiber sensors, two types of flows compete with each other throughout the infusion process, namely, the inter- and intra-roving flow. For the first 6 min, the inter-roving flow dominates and it allows the resin molecules to wet the MWCNT network deposited on outer surface of the fiber roving to result in expansion and even breakage of tube/tube contacts, which causes the significant resistance increase. From 6 min to 28 min, the intra-roving flow dominates. Comparatively, it slowly but continuously penetrates/infiltrates the fiber roving to further disrupt the MWCNT network.

We attribute the rest of the sensor signal to physical/chemical changes in the cross-linking reaction and the concomitant variations of system viscosity, as well as the development of matrix shrinkage caused by phase transformation of gelation and vitrification. Under low levels of cross-linking, the resin molecules retain low viscosity and do not disrupt the equilibrium state of the vacuumed system. As a result, the constant value of dR/R0 from 28 min to 55 min was observed. Continuing with the curing process, sufficiently high levels of cross-linking density would cause a drastic increase of the system viscosity and volumetric shrinkage of the resin. Consequently, the MWCNT network with infiltrated resin shrinks accordingly to cause its conductive paths closing together to have higher packing density. Thus, the substantial decrease of dR/R0 from ~16 to ~4 was observed when the processing time ranges from 1 h to 24 h.

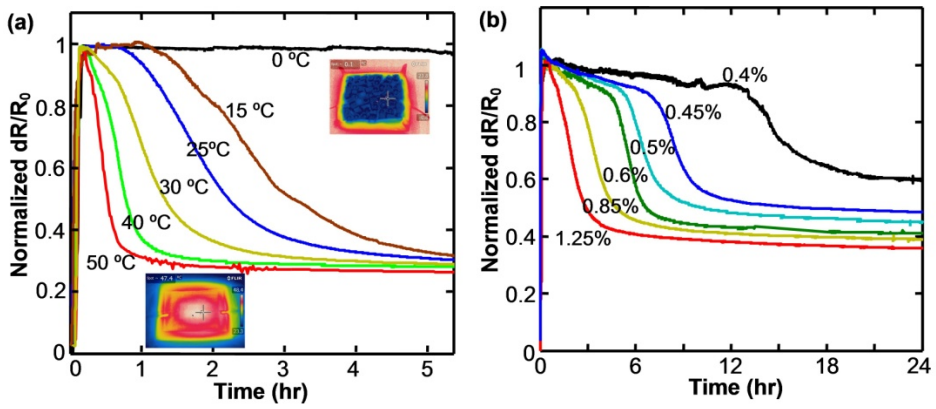

Figure 3. In-line process monitoring of composites using smart fabric method under various (a) curing temperatures and (b) MEKP concentrations.

To better understand the correlation between the sensor signal and cross-linking reaction of the polyester resin, we investigated the effect of curing temperature and resin formulation on the curing process by the results from smart fabric sensor. Figure 3a and 3b respectively show the real-time signals of two series of smart fabric sensors for monitoring the curing process under varied curing temperatures and MEKP concentrations. To better convey the data, the resistance change (dR/R0) was normalized to its maximum value. By keeping the MEKP at 1.25 wt.%, Figure 3a presents a clear trend that for a given resin formulation, the higher the curing temperature, the faster the decay of the sensor signal with respect to the processing time. In addition, as increasing the controlled temperature from 15 °C to 50 °C, the dwelling duration for keeping the highest dR/R0 substantially decreased from~70 min to ~6 min. As another example, the elapsed time for normalized dR/R0 decayed from 1 to 0.5 was decreased from ~120 min (15 °C) to ~25 min (50 °C). It is also interesting that there is a large discrepancy on the final stabilized dR/R0 as the resin formulation is varied. For example, comparing to 0.4 wt.% of MEKP with a stabilized dR/R0 of 0.59, this value drops to 0.33 for 1.25 wt.% of MEKP. This shows a large contrast when compared with the case in Figure 3a, in which all dR/R0 values were stabilized to 0.3±0.05.We argue that the curing temperature only modifies the crosslinking velocity but the resin formation determines not only the curing rate but also the final degree of polymerization.

3.3 Large-area Monitoring of Smart Fabrics

The smart fabric can be easily scaled up to a large sensing network by co-braiding multiple fiber sensors to monitor every local spot of composites. As schematically demonstrated in Figure 4a. During the resin infusion and curing, resistance changes in each horizontal or vertical fiber sensor represent the effect of the resin process near the whole region of the corresponding fiber sensor line. Thus, for a n×m sensor array having "n" horizontal sensors and "m" vertical sensors, the local information near every crossing point (Rij) could be determined by proportionally allocating the relevant horizontal resistance change (RHi) based on all the vertical resistance changes (from RV1 to RVm).The idea is formulated by the following equation defining the resistance change of intersecting points (Rij) in composite laminates with an integrated n×m sensor array in the smart fabric.

$$R_{ij} = \frac{R_{Hi} \times R_{Vj} \times m}{\sum_1^m R_{Vj}} \quad (1)$$

By simultaneously monitoring every horizontal and vertical fiber sensor in the smart fabric, Figure 4b to 4e shows the dR/R0 distribution of each local point at four representative moments of the resin process with a 5×5 sensor array. The optical image in Figure 4b indicates that the resin head was just crossing the fifth vertical sensor line from the right hand side with a curved shape. At this critical

moment, the resistance change of every local point was allocated based on Equation 1. Displaying each resistive value by a three-dimensional bar plot with a color scale, it is amazing that the shape of dR/R0 distribution has faithfully captured the position of the resin head. Clearly, the left 20 points remain unchanged because the resin has not started to wet those regions. In sharp contrast, dR/R0 of the right five points is strongly dependent upon their positions. To specify, the center point experiences the highest dR/R0. With deviating from the center location, the resin head gradually lags behind and the same is true for the resistance change of the corresponding points. Thus, we observed that R55<R45<R35>R25>R15. As the resin head continued to move to the left, Figure 4c and 4d clearly showed that more and more regions were impacted by the resin transfer. A clear gradient of dR/R0 distribution was also found that the longer the region was suffered from the resin infusion, the higher the value of its resistance change. This was caused by the combination of inter-roving and intra-roving flow explained in the previous section. In addition to resin infusion, the dR/R0 distribution during the curing stage was also monitored. Figure 4e shows the corresponding results after three hours of processing. With similar blue-green colors, the magnitude of entire bars fell between ~5 to ~7, indicating that all the local regions were subjected to similar degrees of curing. Based on its ability to map local areas with scalable size and density, we anticipate that the smart fabric technique presented will ensure full cure and no voids in manufacturing high quality composites.

In addition to monitoring the manufacturing process, the smart fabric sensors embedded in composite structures are readily to diagnose its structural health after it is de-molded or debagged. The smart fabric sensors can detect the local stresses or deformations of the composites. The detailed results for this point can be found elsewhere in our newest published work [28]. By applying a compression load, the resistive response of each horizontal and vertical fiber sensor was converted accordingly to dR/R0 values of the local spots based on the same algorithm (Equation 1), the smart fabric sensors can detect the local stresses or deformations of the composites.

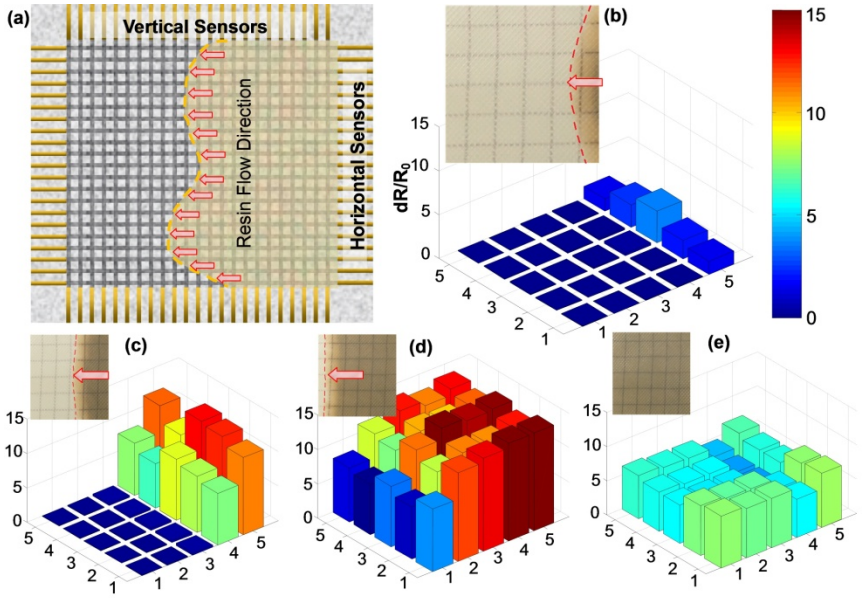

Figure 4. (a) Schematic diagram of the smart fabric including multiple horizontal and vertical sensors for monitoring local information of the real-time resin infusion and curing process; (b-e) Distribution of the resistance change at every local points under different moments of resin infusion and curing by an embedded 5×5 sensor array.

4 CONCLUSIONS

In conclusion, we demonstrated the robust and versatile sensory technology of smart fabric for diagnosing and evaluating the health states of polymeric composites from the manufacturing process to the service stage and finally to failure. By co-braiding MWCNT enabled fiber rovings into a

fiberglass woven preform, we first demonstrated the use of the smart fabric sensor to provide in situ resin infusion and curing information during the vacuum assisted resin transfer molding (VARTM) technique of composite manufacturing. Then, the unique smart fabric sensor readily and noninvasively integrated into the laminate proved to be desirable for monitoring the strain and stress states, as well as for detecting the failures of the host structure. More importantly, the scalable size and adjustable sensing range of the smart fabric allows for covering a laminate of a comparatively large size and also suitable for monitoring the local information of resin processing. The multipurpose sensing capabilities in conjunction with their unique scalability and noninvasiveness make the smart fabric sensor highly valuable for life-long structural health monitoring of high-performance polymeric composites.

ACKNOWLEDGEMENTS

S. Luo gratefully acknowledges the Zhuoyue 100 Talents Plan funded by Beihang University. This work was also jointly supported by National Nature Science Foundation of China (NSFC 11275020), Fundamental Research Funds for the Central Universities (YWF-16-RSC-007), and National Key Research and Development Plan (2016YFC0801906)..

REFERENCES

[1] Boller C, Chang F, Fujino Y. Encyclopedia of Structural Health Monitoring, 1st ed. Wiley: Hoboken; 2009.
[2] Chang F. Structural Health Monitoring 2013 – a Roadmap to Intelligent Structures, 1st ed. DEStech Publications: Lancaster; 2013.
[3] Giurgiutiu V. Structural Health Monitoring of Aerospace Composites, 1st ed. Academic Press: San Diego; 2016.
[4] Konstantopoulos S, Fauster E, et al. Monitoring the production of FRP composites: a review of in-line sensing methods. Express Polym Lett 2014; 8:823-40.
[5] Baughman RH, Zakhidov AA, De Heer WA. Carbon nanotubes – the route toward applications. Science 2002; 297:787-92.
[6] Saito R, Dresselhaus G, Dresselhaus MS. Physical Properties of Carbon Nanotubes, 1st ed. Imperial College Press: London; 1998.
[7] Abot JL, Song Y, Vatsavaya MS, et al. Delamination Detection with Carbon Nanotube Thread in Self-sensing Composite Materials. Compos Sci Technol 2010; 70:1113-9.
[8] Zhang J, Liu J, Zhuang R, et al. Single MWNT-glass fiber as strain sensor and switch. Adv Mater 2011; 23:3392-7.
[9] Kang I, Schulz MJ, Kim JH, et al. A carbon nanotube strain sensor for structural health monitoring. Smart Mater Struct 2006; 15:737-48.
[10] Loh KJ, Kim J, Lynch JP, et al. Multifunctional layer-by-layer carbon nanotube-polyelectrolyte thin films for strain and corrosion sensing. Smart Mater Struct 2007; 16:429-38.
[11] Rein MD, Breuer O, Wagner HD. Sensors and sensitivity: carbon nanotube buckypaper films as strain sensing devices. Compos Sci Technol 2011; 71:373-81.
[12] Wang Z, Xia J, Luo S, et al. Versatile surface micropatterning and functionalization enabled by microcontact printing of poly(4-aminostyrene). Langmuir 2014; 30:13483-90.
[13] Wang Z, Wang J, Xiao Z, et al. A paper indicator for triple-modality sensing of nitrite based on colorimetric assay, Raman spectroscopy, and electron paramagnetic resonance spectroscopy. Analyst 2013; 138:7303-7.
[14] Thostenson ET, Chou TW. Carbon Nanotube Networks: Sensing of Distributed Strain and Damage for Life Prediction and Self Healing. Adv Mater 2006; 18:2837-41.
[15] Gao L, Thostenson ET, Zhang Z, et al. Sensing of Damage Mechanisms in Fiber-reinforced Composites under Cyclic Loading using Carbon Nanotubes. Adv Funct Mater 2009; 19:123-30.
[16] Alamusi, Hu N, Fukunaga H, et al. Piezoresistive strain sensors made from carbon nanotubes based polymer nanocomposites. Sensors 2011; 11:10691-723.

[17] Theodosiou TC, Saravanos DA. Numerical investigation of mechanisms affecting the piezoresistive properties of CNT-doped polymers using multi-scale models. Compos Sci Technol 2010; 70:1312-20.
[18] Nordlund M, Lundstrom TS. An investigation of particle deposition mechanisms during impregnation of dual-scale fabrics with micro particle image velocimetry. Polym Compos 2010; 31:1232-40.
[19] Zhang J, Zhuang R, Liu J, et al. A single glass fiber with ultrathin layer of carbon nanotube networks beneficial to in-situ monitoring of polymer properties in composite interphases. Soft Mater 2014; 12:115-20.
[20] Luo S, Obitayo W, Liu T. SWCNT-thin-film-enabled fiber sensors for lifelong structural health monitoring of polymeric composites – from manufacturing to utilization to failure. Carbon 2014; 76:321-9.
[21] Luo S, Liu T. ACS Graphite nanoplatelet enabled embeddable fiber sensor for in situ curing monitoring and structural health monitoring of polymeric composites. Appl Mater Interface 2014; 6:9314-20.
[22] Luo S, Hoang PT, Liu T. Direct laser writing for creating porous graphitic structures and their use for flexible and highly sensitive sensor and sensor arrays. Carbon 2016; 96:522-31.
[23] Li Y, Luo S, Yang MC, et al. Poisson ratio and piezoresistive sensing; a new route to high-performance 3D flexible and stretchable sensors of multimodal sensing capability. Adv Func Mater 2016; 26:2900-8.
[24] Luo S, Liu T. SWCNT/graphite Nanoplatelet Hybrid Thin Films for Self-temperature-compensated, Highly Sensitive, and Extensible Piezoresistive Sensors. Adv Mater 2013; 25:5650-7.
[25] Luo S, Liu T. Structure-property-processing Relationships of Single-wall Carbon Nanotube Thin Film Piezoresistive Sensors. Carbon 2013; 59:315-24.
[26] Liu T, Luo S, Xiao Z, et al. Preparative Ultracentrifuge Method for Characterization of Carbon Nanotube Dispersions. J Phys Chem C 2008; 112:19193-202.
[27] Luo S, Liu T, Benjamin SM, et al. Variable range hopping in single-wall carbon nanotube thin films: a processing-structure-property relationship study. Langmuir 2013; 29:8694-702.
[28] Luo S, Wang Y, Wang G, et al. CNT Enabled Co-braided Smart Fabrics: A New Route for Non-invasive, Highly Sensitive & Large-area Monitoring of Composites. Scientific Reports 2017.